International Conference on Space Optics—ICSO 2018

Chania, Greece

9–12 October 2018

Edited by Zoran Sodnik, Nikos Karafolas, and Bruno Cugny

An optically athermalized lens covering a 200-degree temperature range

John Rogers

International Conference on Space Optics — ICSO 2018, edited by Zoran Sodnik, Nikos Karafolas, Bruno Cugny, Proc. of SPIE Vol. 11180, 111808E · © 2018 ESA and CNES · CCC code: 0277-786X/18/$18 · doi: 10.1117/12.2536221

An optically athermalized lens covering a 200-degree temperature range

John R. Rogers

Synopsys, Inc.

ABSTRACT

There are several methods for athermalizing an optical system. Active athermalization requires that the focus of the system be actuated as a function of temperature. This adds complexity to the system and is often not desired for Space applications. Mechanical athermalization does not attempt to stabilize or otherwise influence the optical behavior over temperature, but relies on a mount structure that is engineered to keep the focal plane array (FPA) located at the position of best focus over temperature. Often such mounts involve dissimilar materials expanding in opposite directions to obtain the desired net expansion. Optical athermalization keeps the mount structure simple but uses a modified optical design to ensure that the position of best focus falls at the FPA location across the temperature range. To achieve this while still producing a sharp image, the lens materials must be chosen carefully.

In designing an athermalized lens, the mounting details of the elements must be taken into account carefully. A common approach for optimization is to assume that the elements are separated by spacers whose CTEs are known. Unfortunately, in most cases this is not how the optical system is actually assembled. More commonly, the individual lenses are either cemented to or otherwise preloaded against seats cut into the housing barrel. Furthermore, there are many ways in which the contact between the optical elements and the housing takes place, and this influences the location where each element is "pinned" to the housing, i.e., the position at which there is no relative motion between the element and the housing.

In this paper, we present the design of a lens optimized to be optically athermalized over a 200° C temperature range. The design includes the effects of the lens mounting details as well as the change in CTE of aluminum over temperature. We also explore the sensitivity of the design to the mounting details and the CTE.

Keywords: passive athermalization, optical design

1. INTRODUCTION

The traditional method of calculating and compensating for thermal effects in optical systems, in use as recently as recently as 2009, is to work with equations that relate the thermo-optical coefficients (dn/dT values) and the coefficients of thermal expansion (CTEs) of both the housing and the lens elements to the state of focus at the FPA[1-3]. While this approach remains valid, it is difficult to apply to a system involving many elements, and – since it considers only first order properties – it ignores the change in aberration with temperature. A better approach is to model and optimize the system at multiple temperatures that span the operational range of temperatures for the system.

In such a model, it is important that the interaction of the optical elements with the housing be taken into account accurately. It is not sufficient merely to assume that the elements scale according to their CTE values, and that the spaces between them scale according to the CTE of the housing. This is because spaces between optical elements are typically defined as the distances between the on-axis vertices of the elements, whereas the elements are actually held apart by the contact of their *edges* with the housing. The separations of the lens edges are often very different than the separations of the vertices, as the lens shown in Figure 1 demonstrates.

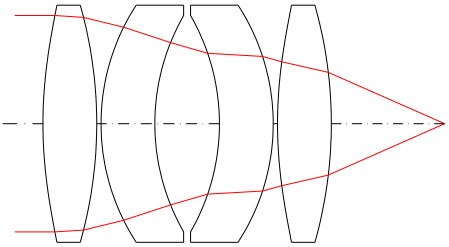

Figure 1. Lens demonstrating differences between vertex separations and edge separations

It is useful to note that calculating expansion based on an incorrect thickness is equivalent to using the correct thickness with an incorrect value of the CTE. Our experience with a similar lens was that the CTE value of the housing had a much stronger influence on the thermal stability than the CTE values of the glasses, or the dn/dT values of the glasses[4]. This is equivalent to stating that the air spaces used in the housing expansion calculations must accurately reflect the edge separations rather than the vertex separations of the elements.

A better, though often still inadequate, approach is to assume that the elements are held apart by spacers that contact the elements outside their clear apertures, as shown schematically in Figure 2. In this concept, the positions of the elements depend not only on the expansion of the spacers, but also on the expansions of the other lens elements in the system. Done carefully, this approach can be accurate for systems that are assembled using the "elements and spacers in a tube" approach.

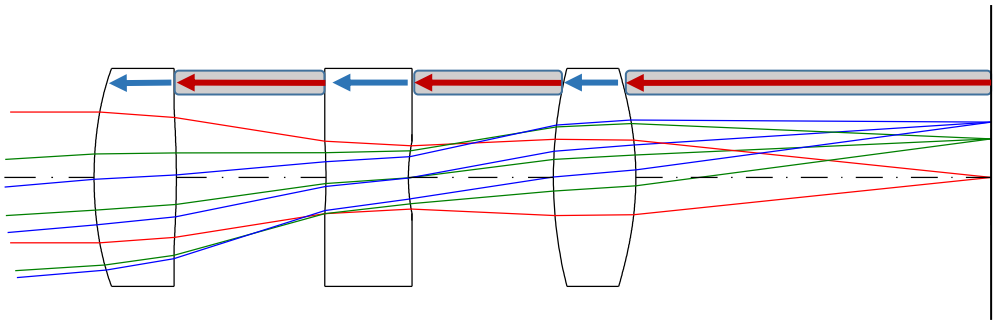

Figure 2. Expansion diagram, loose elements and spacers, showing the expansion of spacers in red and the expansion of lens elements in blue.

To model this kind of an assembly accurately, it is necessary to model not only the longitudinal expansion of the spacers and lens elements, but their transverse expansions as well. If the spacers (which are typically metallic cylinders) expand more rapidly than the lens elements, then they contact the lens elements at positions farther from the optical axis; at these locations the lens elements are either thicker or thinner than at the nominal contact points, and this causes longitudinal shifts of the elements.

Most optical systems designed for Space applications involve lenses that are either cemented to, or preloaded against, precisions seats cut into a monolithic or at least piecewise monolithic barrel or housing, as shown schematically in Figure 3. In this case, the locations of the reference (seated) surfaces of the lenses depend only on the expansion of the housing material, and the locations of the "floating" surfaces of the elements can in some cases move in the opposite direction relative to the reference surface.

Although it may seem that the differences between the expansion models shown in Figures 2 and 3 are small, they are not negligible for applications in which the temperature range is large and/or the depth of focus is small.

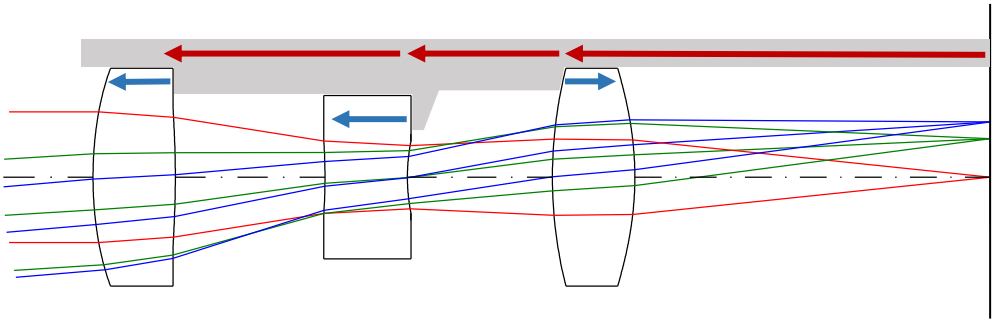

Figure 3. Expansion diagram, elements cemented to housing seats, showing the expansion of spacers in red and the expansion of lens elements in blue.

In any optically athermalized design, the choice of glass types is extremely important, because the properties of the glass determine not only the degree to which the lens is corrected for chromatic aberration, but the rate of focal shift change with temperature as well. For this reason, glass choice is especially important when the optical design must operate over a wide spectral band and a wide temperature range.

Expansion coefficients for most optical glasses are in the range of a few parts per million (ppm) per degree Celsius. Taken by itself, this effect causes lenses to lengthen in focal length by a few ppm/ºC as they are warmed. On the other hand, in the visible region of the spectrum, most optical glasses have a thermo-optical coefficient that is positive, meaning that the index (somewhat counter-intuitively) *increases* with increasing temperature. There are exceptions, but this effect generally tends to *shorten* the focal length by a few ppm/ºC as the system is warmed. In most cases of systems whose glass types are selected for optimal performance at room temperature, the net effect is that the system focal length increases slightly with temperature. On the other hand, the housing generally has a much larger expansion coefficient than glass, and larger also than the combined effect of glass expansion and dn/dT. Aluminum has a CTE of about 23 ppm/ ppm/ºC, for example. As a result, the housing tends to push the FPA away from the optics faster than the focal length and the optical back focal distance are expanding.

One common approach for dealing with this unfortunate mismatch is mechanical athermalization, i.e., designing the housing in a clever way to match the behavior of the optics. Usually, this involves the use of two concentric sleeves of dissimilar materials expanding in opposite directions in such a way that the net expansion matches the drift of focus of the optics.

The approach taken here is to leave the housing simple, and select the lens materials in such a way that the change in back focal distance with temperature matches the behavior of the housing. To accomplish this, we use a multiconfiguration model of the optical system that simultaneously represents several temperatures, and we allow the automated glass selection algorithm of CODE V to select glasses that reduce the optical aberrations over temperature.[5] Despite the fact that glasses must be chosen to simultaneously satisfy the requirements of both color correction and athermalization, we have found that in most cases there is sufficient diversity of glass types to allow this to be done.

2. INITIAL ROOM-TEMPERATURE DESIGN

To demonstrate this technique, we selected the following specifications, which are typical of those that might apply to an optical system for a planetary lander, but are not specific to any particular program:

- Focal length at λ=675 nm: 100 mm
- F/2.8
- Image circle diameter 16.392 mm (full field of view 9.37º)
- Pixel pitch 0.005 mm (Nyquist frequency 100 cy/mm)
- First element to be radiation-resistant glass

- Remaining elements to be commercially-available glass types, Fused Silica, or CaF2
- Operating temperature range: -80ºC to +120ºC
- Operating pressure: Zero (vacuum)
- Wavelengths in nm (and weights): 900 (56%), 788 (100%), 675 (89%), 563 (78%), 450 (33%)
- Bandpass filter substrate: 3 mm fused silica
- Detector cover glass: 0.55 mm thick, modeled as Schott K10
- Housing material: 6061 T6 Aluminum

To begin the design process, we created a four-configuration model of a ten-element starting lens. The four configurations (or "zoom positions" in the language of CODE V) represent:

1. The fabrication and alignment condition of 22ºC and 760 mm Hg
2. The cold in-use condition of -80º C and 0 mm Hg
3. The middle in-use condition of 22º C and 0 mm Hg
4. The hot in-use condition of +120º C and 0 mm Hg

As a starting point, we chose a 10-element design, shown in Figure 4, that was optimized for ordinary laboratory conditions of 22º C and 760 mm Hg. We have listed the glass types on the drawing because the evolution of the glass selection turns out to be crucial to the success of the design.

This initial design performs fairly well at the design conditions. Figure 5 shows the Modulation Transfer Function (MTF) out to the Nyquist frequency of 100 cy/mm.

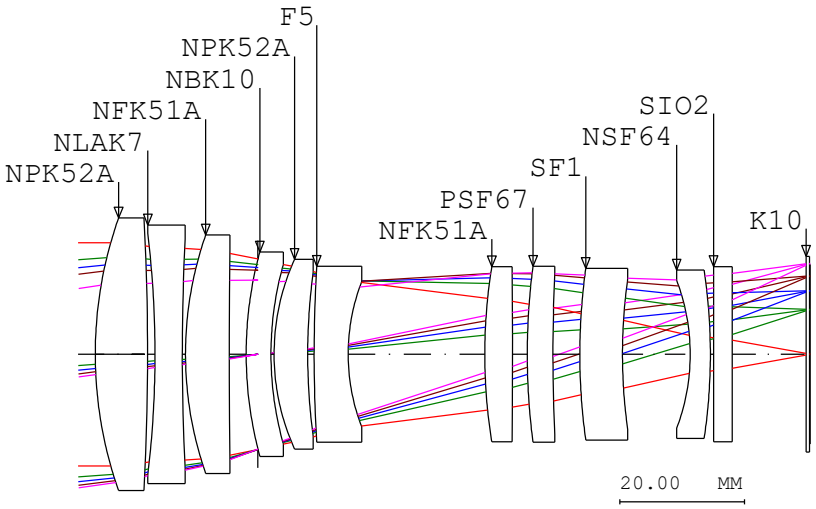

Figure 4. Room-temperature, 10-element starting point

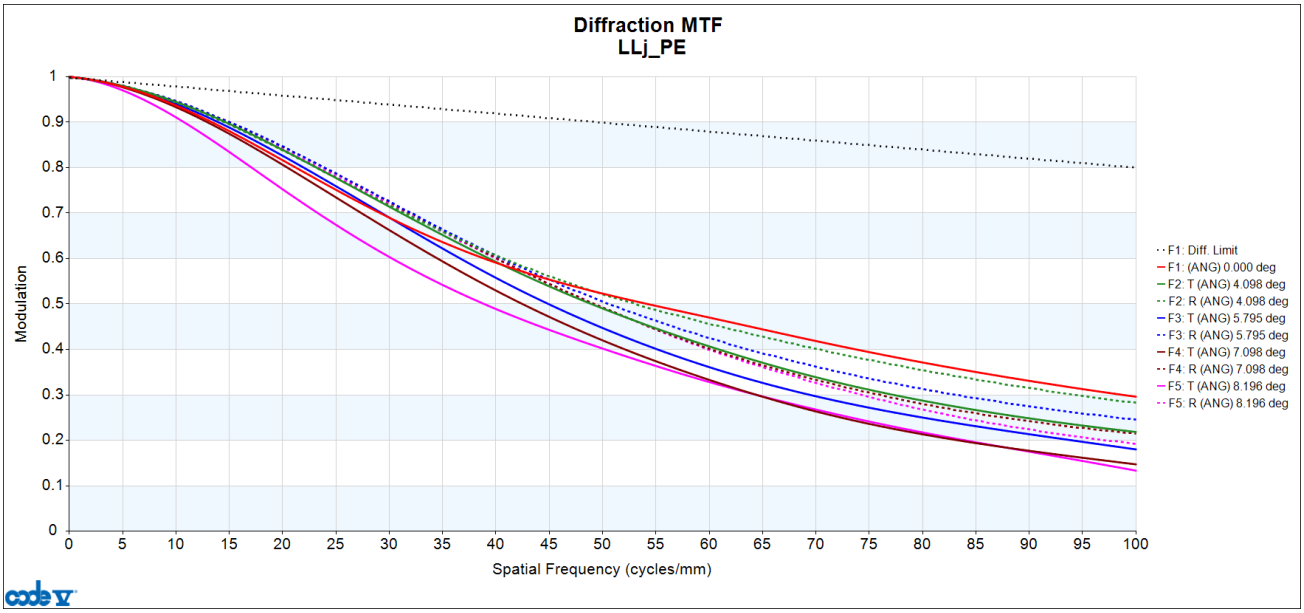

Figure 5. MTF of the design of Figure 3; T = 22 º C, P = 760 mm Hg

In constructing the three in-use configurations, we took into account the CTE values of the glasses as well as the thermally-induced changes in their refractive indices. This latter property is not simply determined by a single dn/dT value, but determined by an expression (measured by the glass manufacturers) that varies with the second power of the temperature and the first power of the wavelength. For the housing expansion, we used a model, derived from data from the U.S. National Institute for Standards and Technology (NIST), in which the change in length per unit length is cubic with temperature. This yields a CTE value that varies quadratically with temperature.[6]

At the in-use conditions of zero pressure and temperatures of -80º C, +22º C, and +120º C, the performance is much worse, as evidenced by Figures 6, 7, and 8.

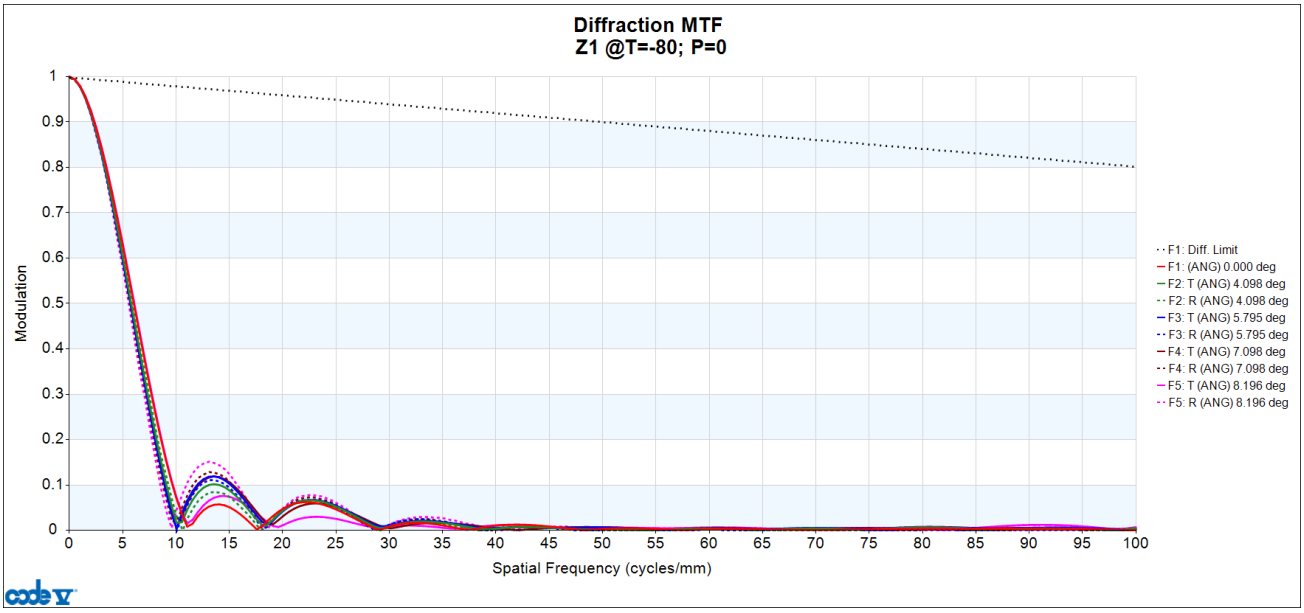

Figure 6. MTF of the design of Figure 3; T = -80 º C, P = 0 mm Hg

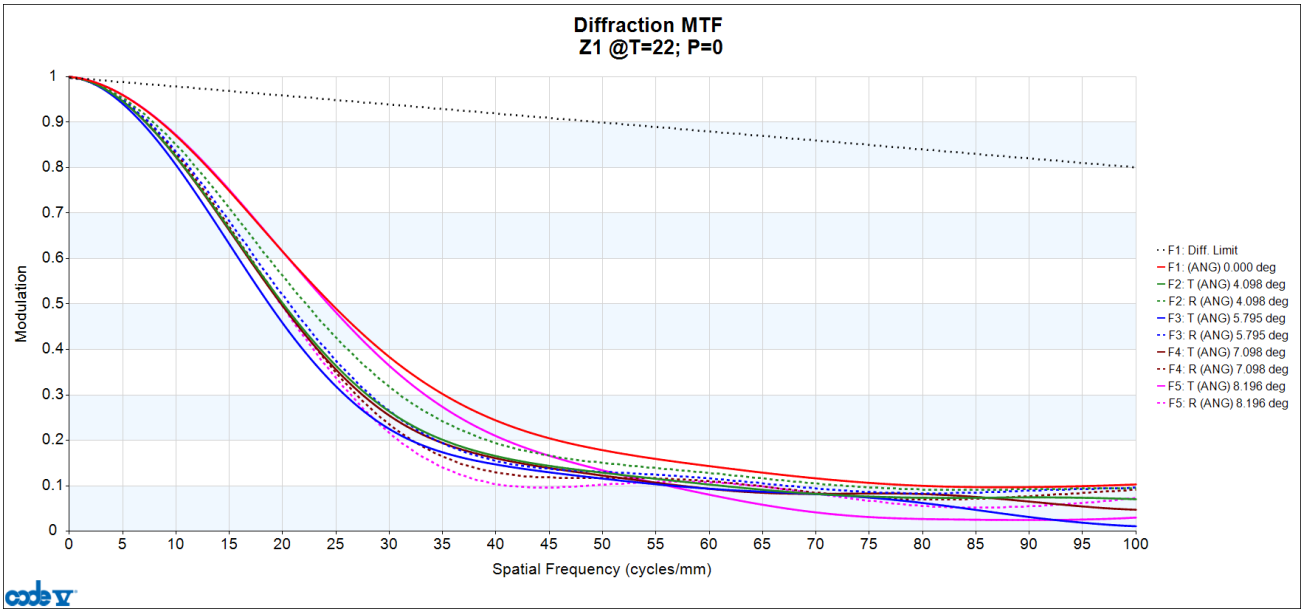

Figure 7. MTF of the design of Figure 3; T = 22 º C, P = 0 mm Hg

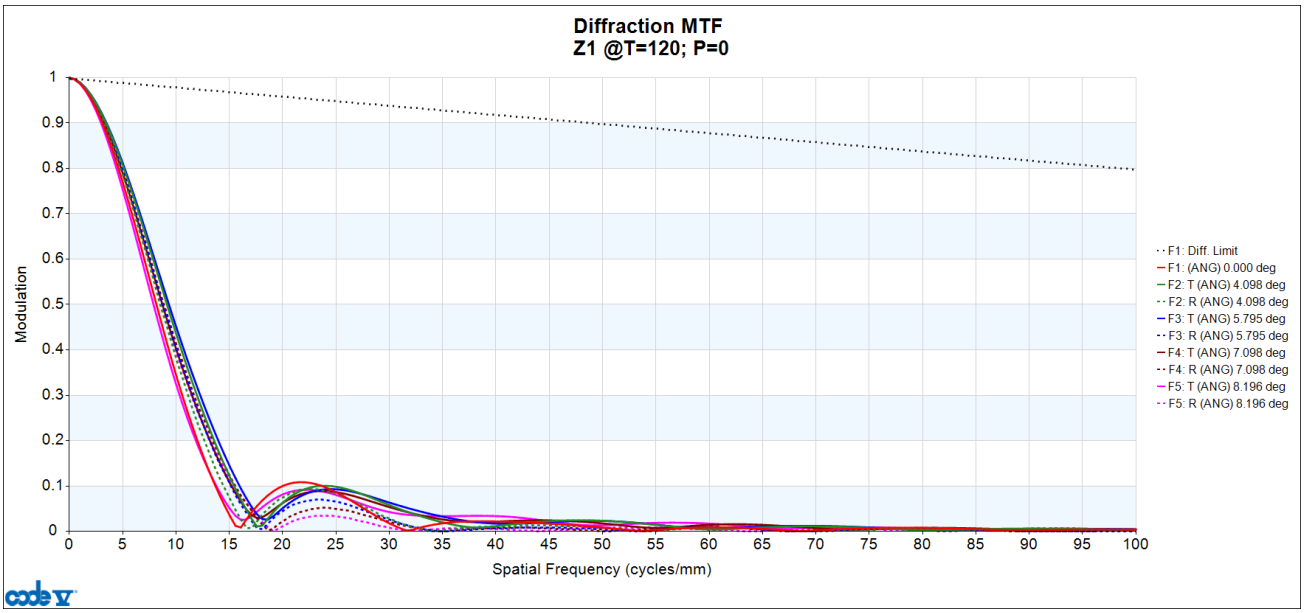

Figure 8. MTF of the design of Figure 3; T = 120 º C, P = 0 mm Hg

The performance in Figure 7 is noticeably better than in Figures 6 and 8 (though still worse than in Figure 5). This is because the temperature is the same for Figures 4 and 6; thus the sole reason for the performance drop is the change in pressure. For Figures 5 and 7 the temperature shifts in addition to the pressure shift.

3. INITIAL OPTIMIZATION FOR THE IN-USE CONDITIONS

We optimized the design shown in Figure 4 simultaneously for four "zoom positions" representing the nominal fabrication conditions plus the three in-use conditions whose MTFs are depicted in Figures 6 – 8. Because we really only care about the performance of the system in the in-use conditions, we set the relative optimization weight for the first zoom position to be very low relative to the in-use positions 2 – 4. (Even though we don't care about the performance of the system at the first zoom position, it is useful to keep that position in the lens model, because in the end, it will be the design prescription that is to be given to the fabricator.)

In this optimization, we allowed the glass types of all elements except for the filter substrate and the detector window to change. More specifically, we used the Glass Expert feature of CODE V (which is normally used to correct chromatic aberration) to search for glass types that improve the performance across temperature. It is worth noting that at this point we allowed unconstrained substitution of the glass type for the first element, even though we know that we will eventually want a radiation-resistant glass for the front element. There are many kinds of radiation-resistant glasses, spanning a wide range of refractive indices and dispersion (Abbe) values. Rather than guess at what glass type to insert for the front element, we allowed the optimizer to find a solution, with a plan of later substituting a radiation-resistant glass with similar properties.

The design resulting from this optimization is shown in Figure 9. Comparing this to Figure 4, we can see that the glass type of every lens element has changed. Figures 10-13 show the MTF of the reoptimized system. Now, the performance at the nominal, laboratory condition is poor (because the system is strongly out of focus), but the MTF at the in-use conditions is good at all three temperatures.

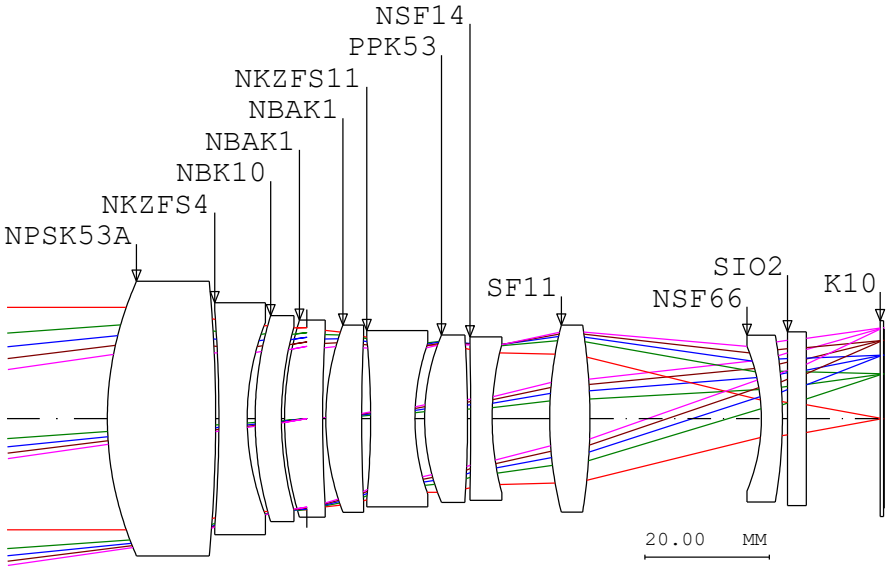

Figure 9. Athermalized version of the Figure 3 design

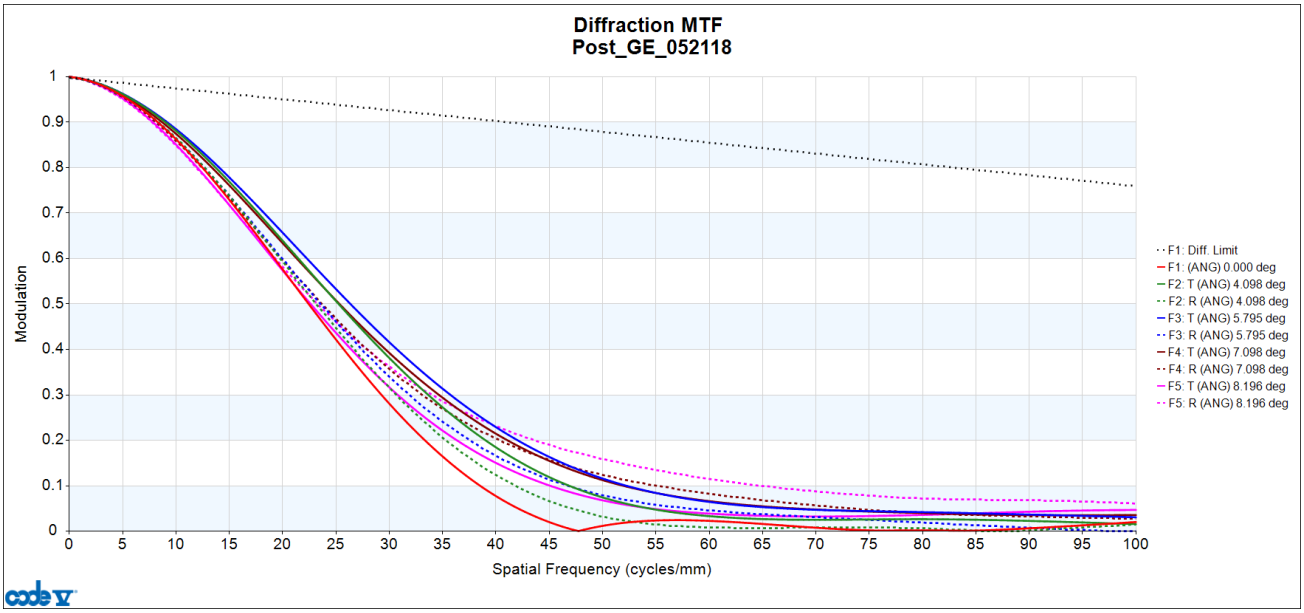

Figure 10. MTF of the design of Figure 8 at 22° C and 760 mm Hg.

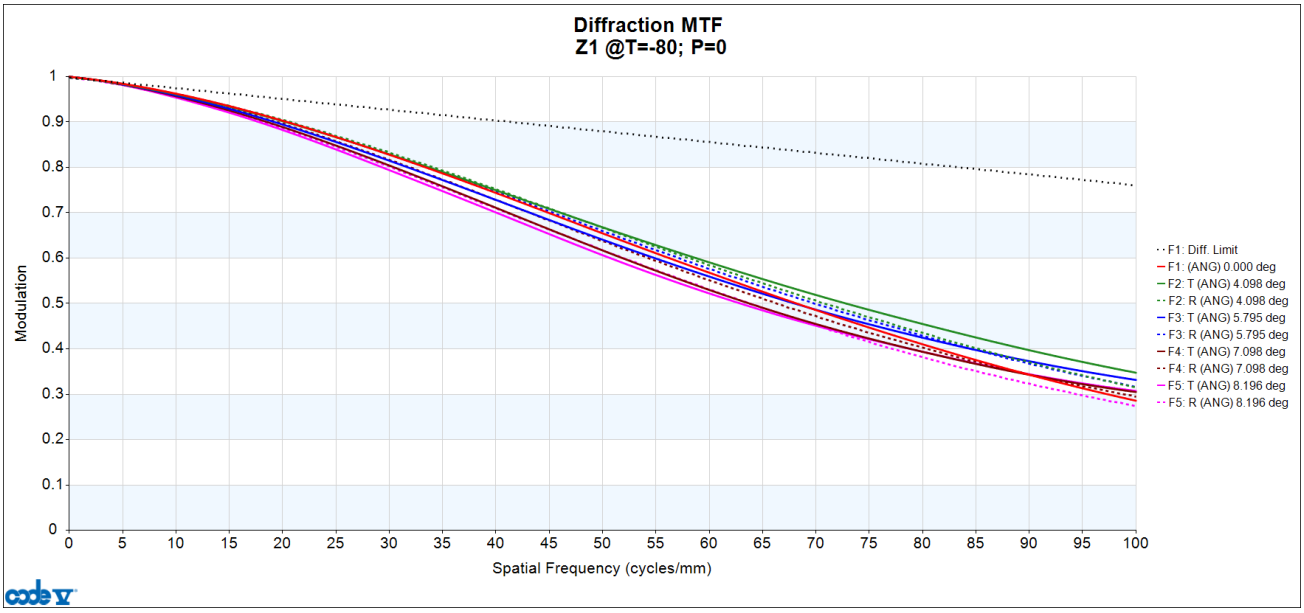

Figure 11. MTF of the design of Figure 8 at -80° C and 0 mm Hg.

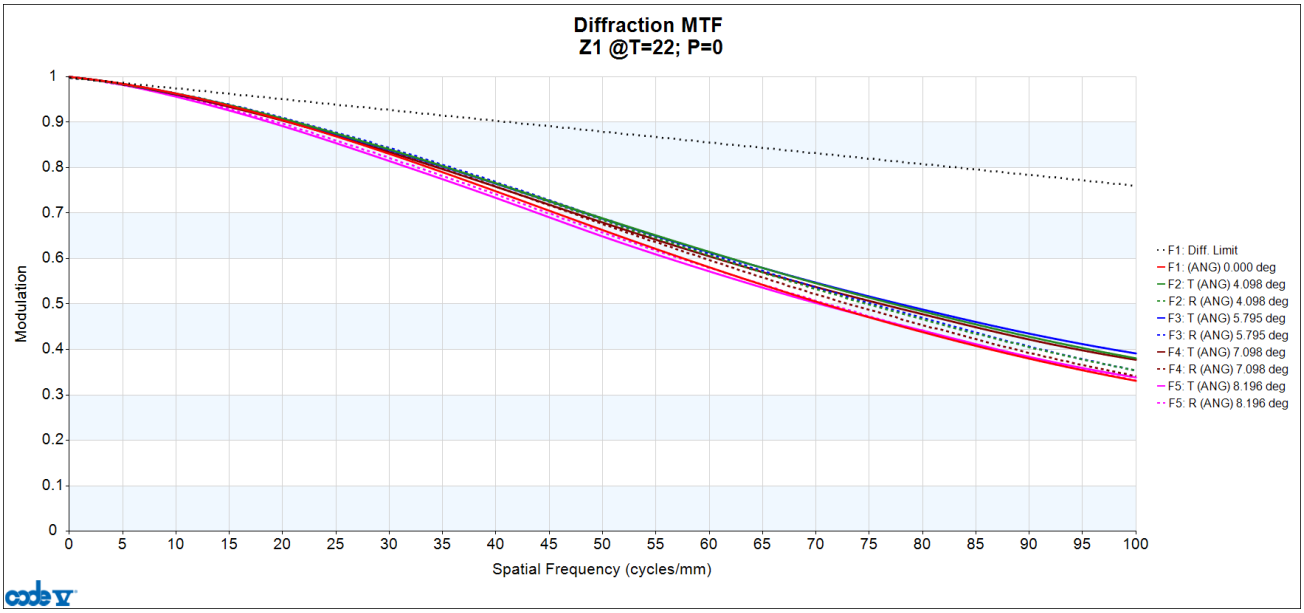

Figure 12. MTF of the design of Figure 8 at 22º C and 0 mm Hg.

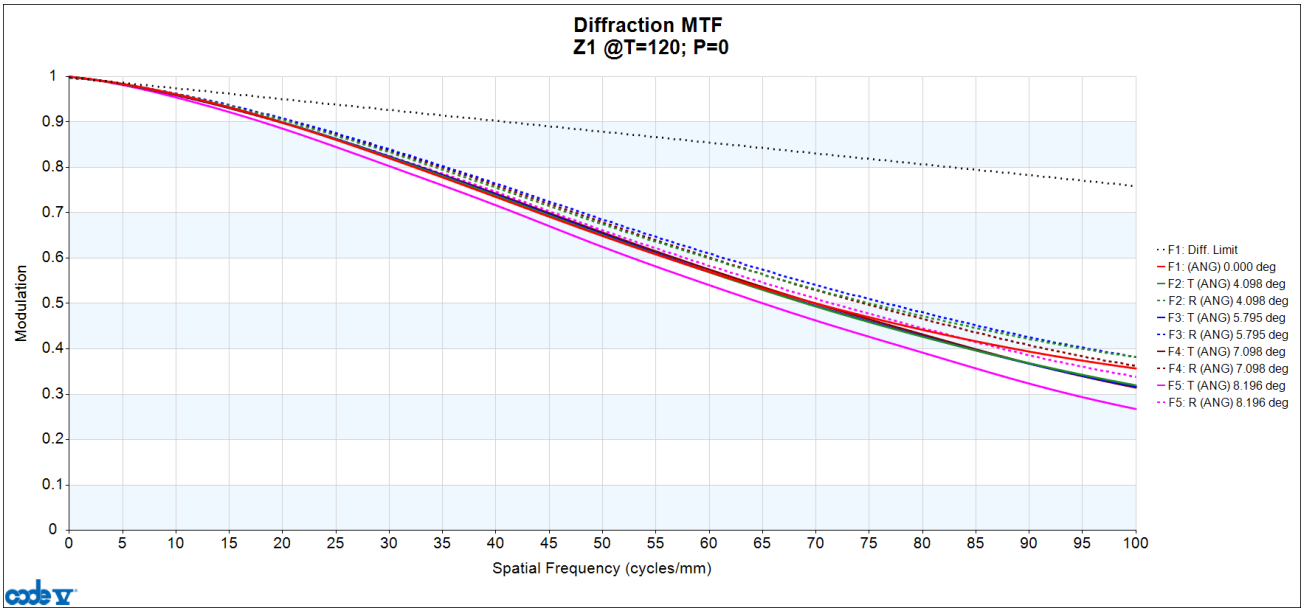

Figure 13. MTF of the design of Figure 8 at 120º C and 0 mm Hg.

4. FURTHER OPTIMIZATION FOR THE IN-USE CONDITIONS

Although the design shown in Figure 9 performs very well at the in-use conditions, the third element is extremely weak and contributes almost nothing to the correction of the aberrations. For this reason, we removed the third element from the model and reoptimized. The resulting design, shown in Figure 14, performed nearly as well as the design of Figure 9.

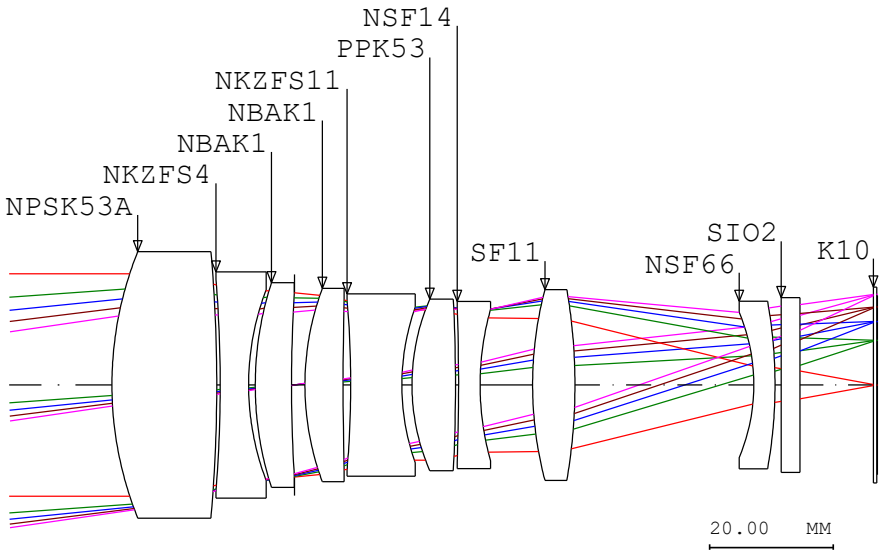

Figure 14. Athermal nine-element design, with unconstrained glass types

Next, we address the problem of the first element, which is a glass from Schott that is not radiation resistant. This is not surprising, since we allowed the front glass to be substituted freely during the previous optimizations. NPSK53A has a moderately high index and a high Abbe number. Of the radiation-resistant glasses, the closest match to this is the Ohara glass SBSM22R. We therefore changed the glass type of the first element from NPSK53A to SBSM22R for the next optimization.

At the start of this next optimization, we had some concerns about secondary color correction, since we had just replaced a glass that had particularly good secondary color properties with a glass with secondary color properties that are much more ordinary. Nevertheless, resulting lens, shown in Figure 15, also was well corrected for secondary color, and was also well corrected over temperature. It is worth noting that between Figures 14 and 15, in addition to the front glass, several other glass types have changed. The design was able to recover from the loss of PSK53A, and it did so by swapping in other glasses (such as NFK51A) that are advantageous for the correction of secondary color. The MTF curves for the Figure 15 design are nearly identical to Figures 9-12, and not included here.

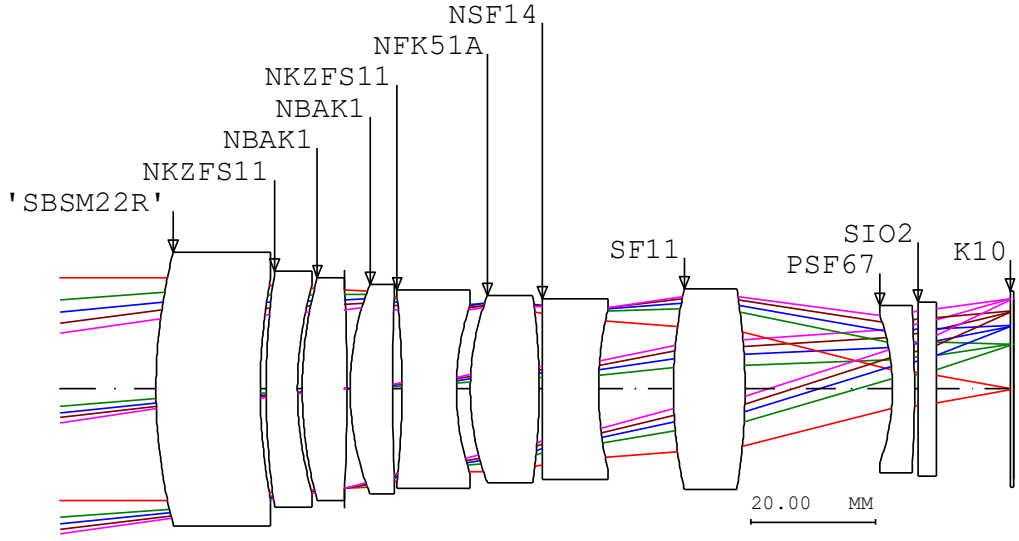

Figure 15. Revised design with radiation-resistant front element.

The design form shown in Figure 15 suffers a hidden problem. Initially, we had constructed the lens model under the assumption that the housing would be an "hourglass" shape, with roughly half the elements loaded from the left, and the other half (including the filter and the detector assembly) loaded from the right. As the design evolved, the location of the element with the smallest diameter changed. Periodically, we updated the seating plan for the model to accurately reflect the sides of the lenses that would likely be cemented to the housing. For the last several optimizations, (beginning with Figure 9), the seventh element has been the smallest.

Once we began to consider in detail what the assembled lens might look like, it became evident that the stated arrangement would likely be problematic. If we make the seventh element only as large as it needs to be, and then require that the sixth element be modestly larger (for instance, two millimeters on a radius) in order to have an adequate seating surface, and continue to make each element larger as we work our way toward the front of the objective, it becomes evident that the front element would need to be significantly larger and heavier than would be required for purely optical reasons. In addition, some collisions would occur as the elements were enlarged, for instance between Elements 1 and 2. For this reason, we revised our housing concept to that shown schematically in Figure 16.

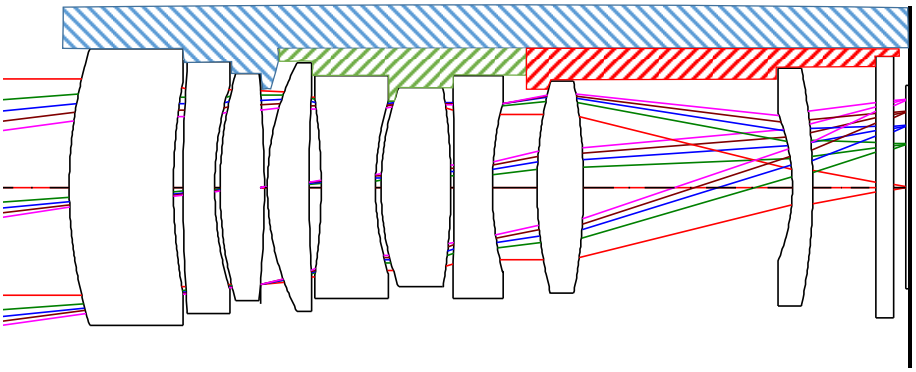

Figure 16. Three-part housing concept

In this concept, the first three elements would be loaded into the main housing from the left. The next four elements would be loaded into a sub-cell, two from the left and two from the right. The sub-cell would be loaded from the right into the main housing. Finally, the last two lens elements plus the filter substrate would be loaded into a different sub-cell from the right, and that sub-cell loaded into the main housing from the right. The use of sub-cells is not to take advantage of the possibility of using dissimilar materials – we have assumed that all three parts of the housing are 6061 T6 aluminum – but merely to develop a seating plan that does not require the elements to grow monotonically larger as one moves toward the front of the objective. This housing concept reverses the seats on Elements 6 and 7: previously they were seated on their right sides, and now they are seated on their left sides.

Changing the seating surfaces for Elements 6 and 7 had a minor effect on the thermal stability of the system. Even though the effect was small, we elected to reoptimize the system for the modified seating plan. Accordingly, we modified the lens model to represent the updated seating sides of Elements 6 and 7 and reoptimized, once again allowing new glasses to be chosen except for the front element, which was "frozen" as SBSM22R. The resulting lens is shown in Figure 17. It is worth noting that even the small modification of changing the seating surfaces of two elements caused the optimum glass choice for one element to be changed. The prescription data (at the fabrication temperature and pressure) for this lens are listed in Table 1.

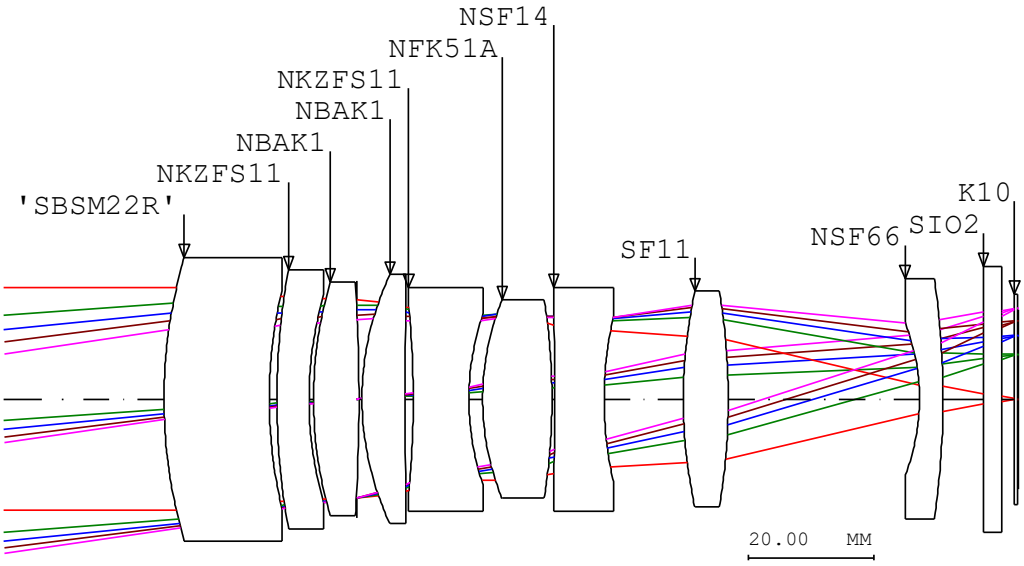

Figure 17. Lens after reoptimizing with corrected seat orientations.

Table 1. Fabrication Prescription (at T = 22°C, P = 760 mm Hg) for the design of Figure 16

Surface	Radius (mm)	Thickness to Next	Glass Type
1	78.904	16.918	SBSM22R_OHARA
2	78.550	1.193	
3	118.739	5.172	NKZFS11_SCHOTT
4	60.519	0.753	
5	67.418	7.144	NBAK1_SCHOTT
6	-353.871	-0.355	
7 (Stop)	INF	0.855	
8	47.955	6.775	NBAK1_SCHOTT
9	536.981	1.441	
10	-141.468	8.814	NKZFS11_SCHOTT
11	43.782	1.263	
12	42.867	11.113	NFK51A_SCHOTT
13	-105.722	0.500	
14	-2288.639	7.694	NSF14_SCHOTT
15	63.140	13.502	
16	84.207	10.449	SF11_SCHOTT
17	-114.695	27.976	
18	-35.007	3.852	NSF66_SCHOTT
19	-164.980	6.895	
20	INF	3.000	SIO2_SCHOTT
21	INF	2.000	
22	INF	0.550	K10_SCHOTT
23	INF	0.089	
24 (Image)	INF	N/A	

The MTF of the design shown in Figure 17 is shown in Figures 18 – 20 for the in-use conditions. The performance is very stable across temperature.

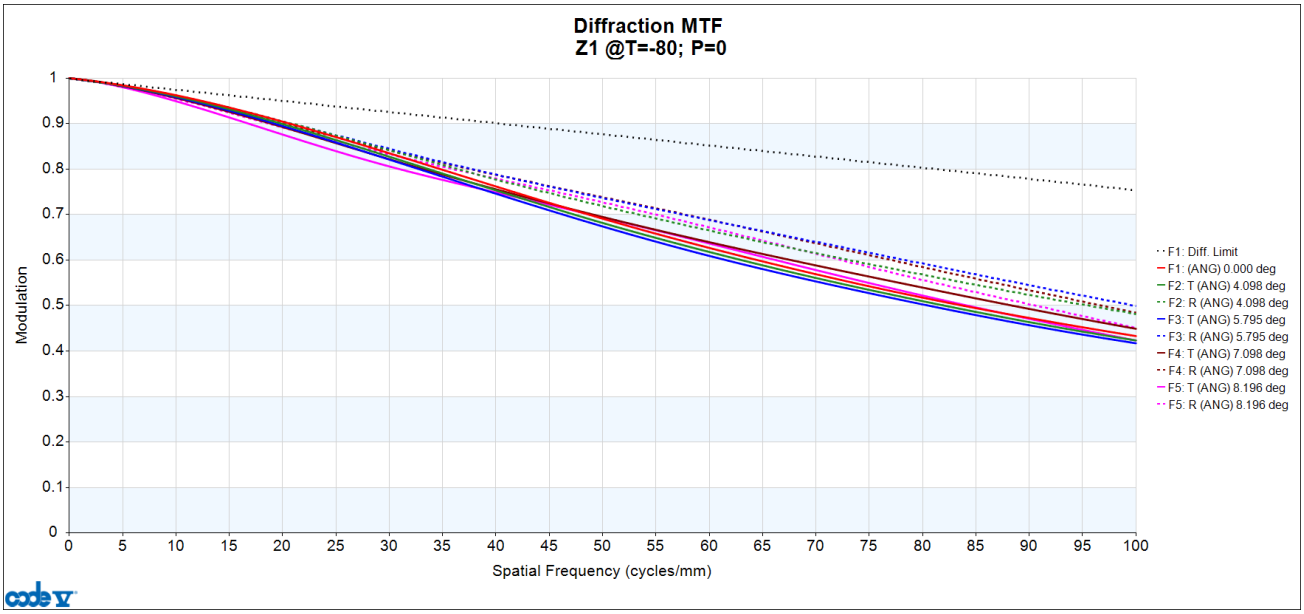

Figure 18. MTF of the design of Figure 16; T= -80, P = 0 cy/mm

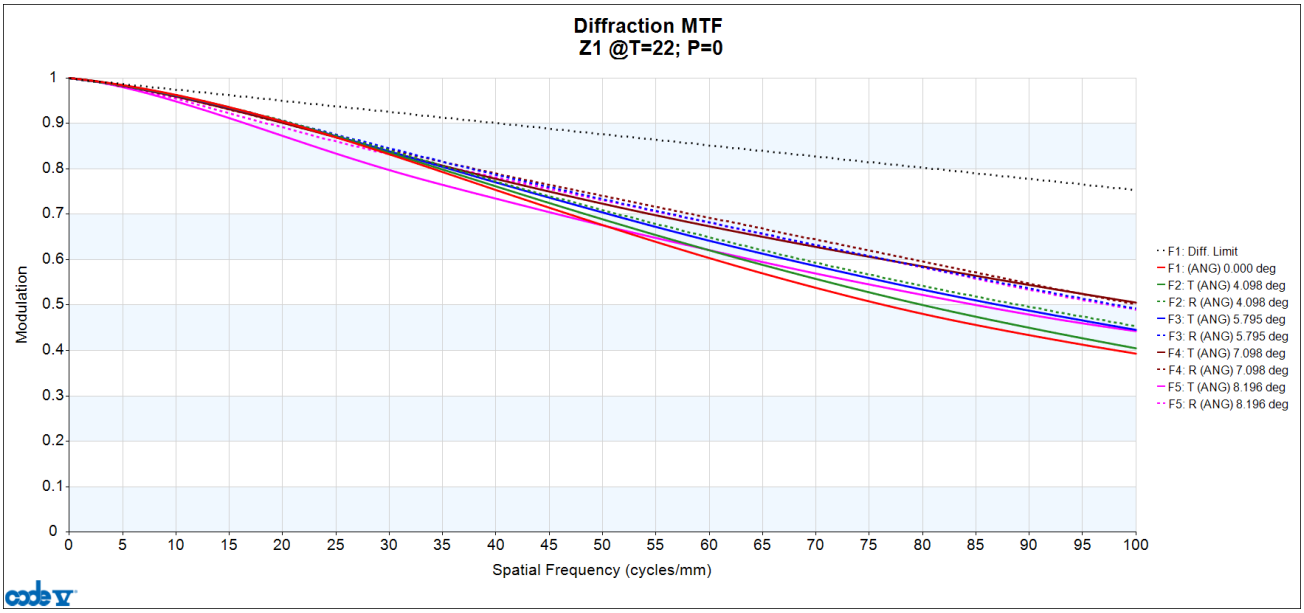

Figure 19. MTF of the design of Figure 16; T= 22, P = 0 cy/mm

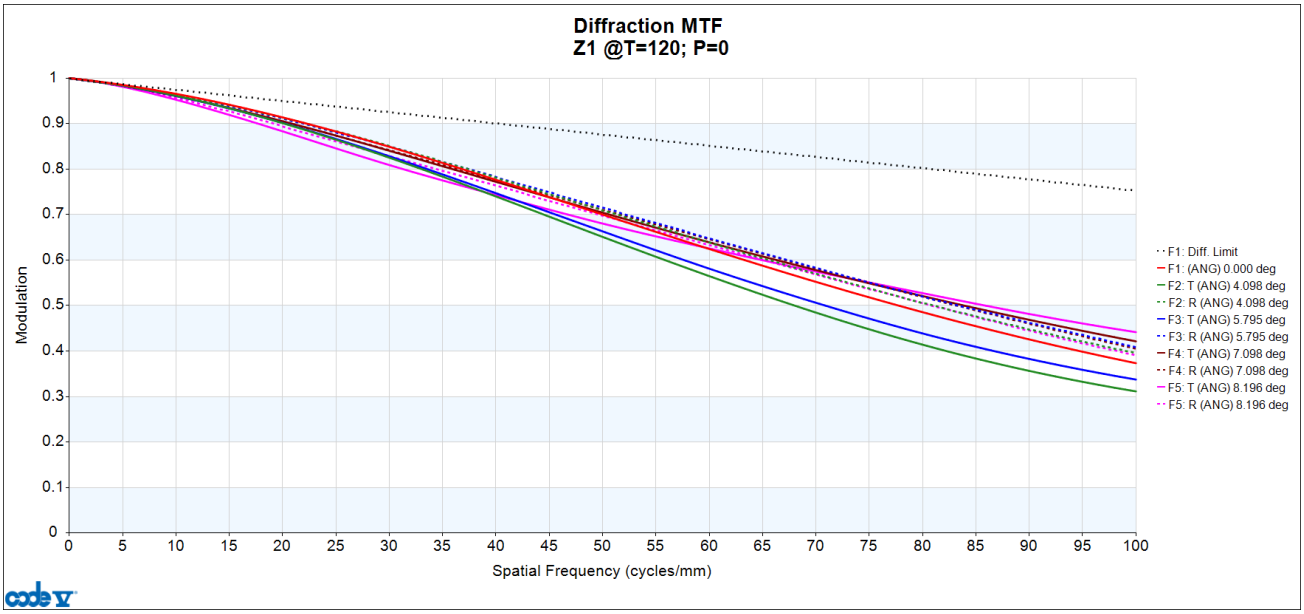

Figure 20. MTF of the design of Figure 16; T= 120, P = 0 cy/mm

5. SENSITIVITY TO MOUNTING DETAILS

In the optimization and analysis carried out above, we assumed that the elements are seated against the housing just outside their clear apertures. More precisely, we assumed that convex surfaces are seated directly against the housing, and that in the case of concave surfaces, it is the edge flat outside the clear aperture that contacts the seat. We did the analysis this way because this is the most common way of mounting high precision elements; however, other assumptions are possible. The modeling software allows us to apply a longitudinal offset between the housing seat and the position of the edge of the optical surface. This capability is intended to cover cases in which a ledge is ground into the edge of a thick part, and cases in which the edge of the part is made thicker outside the clear aperture (as is commonly done with plastic optics). Another interesting situation is that in which the elements are cemented to the housing with a bead of cement running around their edge cylinders. In this case, the most logical assumption is that the center of the cement bead is the position where there is no relative motion between the element and the housing, as Figure 21 illustrates.

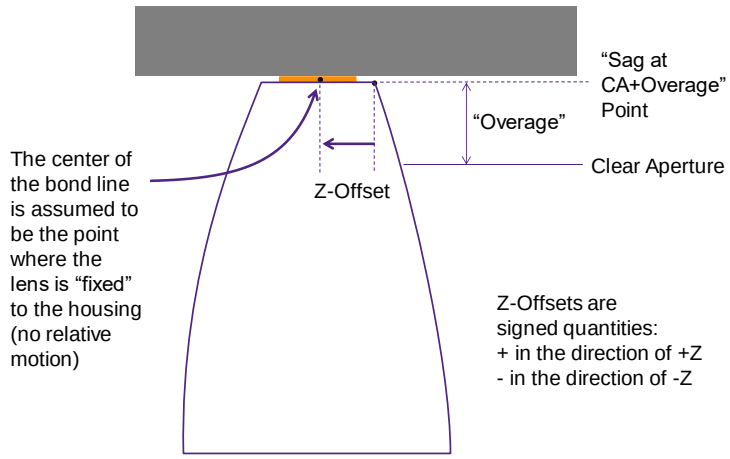

Figure 21. Edge cementing of an optical element represented by a Z-offset from the optical surface

Here, we investigate what happens to the performance of the system if it is designed for seat mounting (as in the foregoing sections of this paper), but the manufacturer decides the mount the elements according to Figure 21 without reoptimizing the design. This simple test will give an indication of how sensitive the thermal properties of the system are to the details of how the lens edges interact with the housing.

To carry out this test, we simply apply a Z-offset equal to every element, equal to half the edge thickness of that element. In the design of Figure 16, the first five elements are mounted on their second sides, so the Z-offsets for those elements are negative, while the Z-offsets for the remaining elements are positive in sign. With the offsets applied, we recalculate the MTF curves for the in-use conditions; those are shown in Figures 22-24.

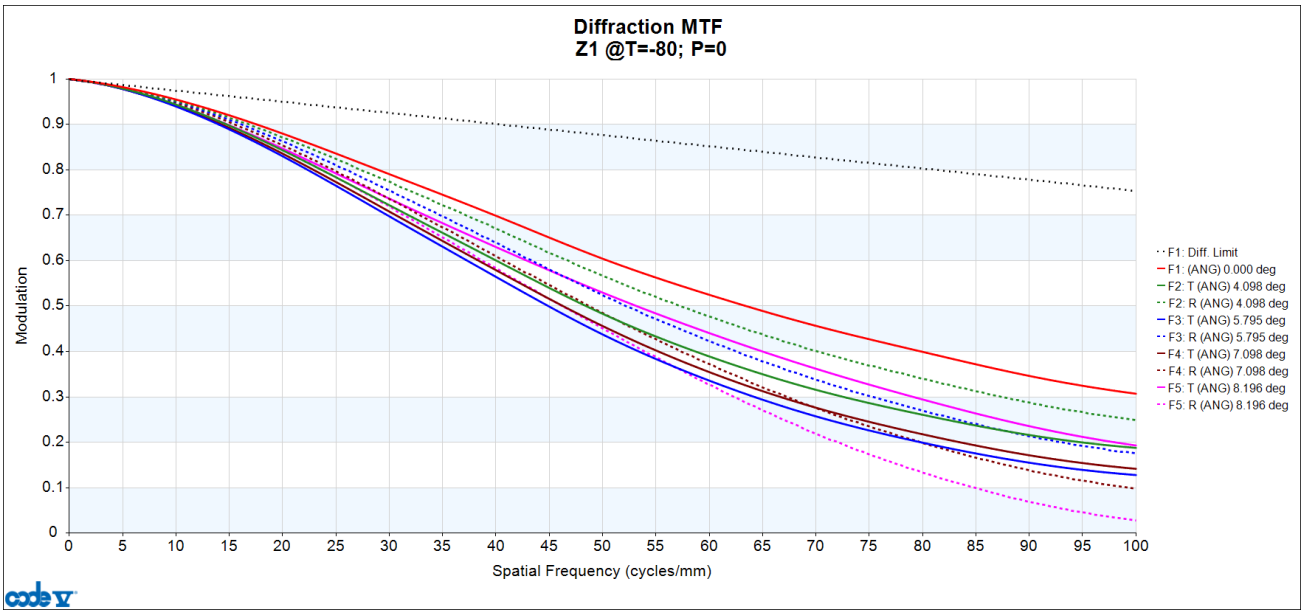

Figure 22: MTF (at T= -80, P = 0 mm Hg) for the design of Figure 16, assuming edge-cementing of elements.

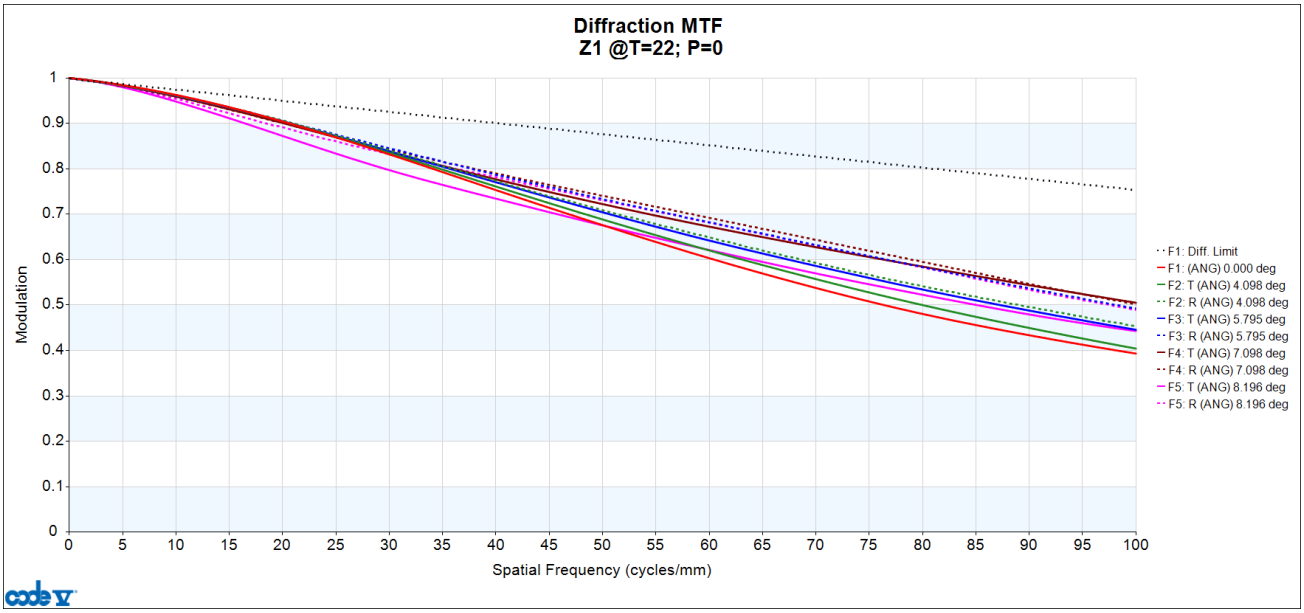

Figure 23: MTF (at T= -80, P = 0 mm Hg) for the design of Figure 16, assuming edge-cementing of elements.

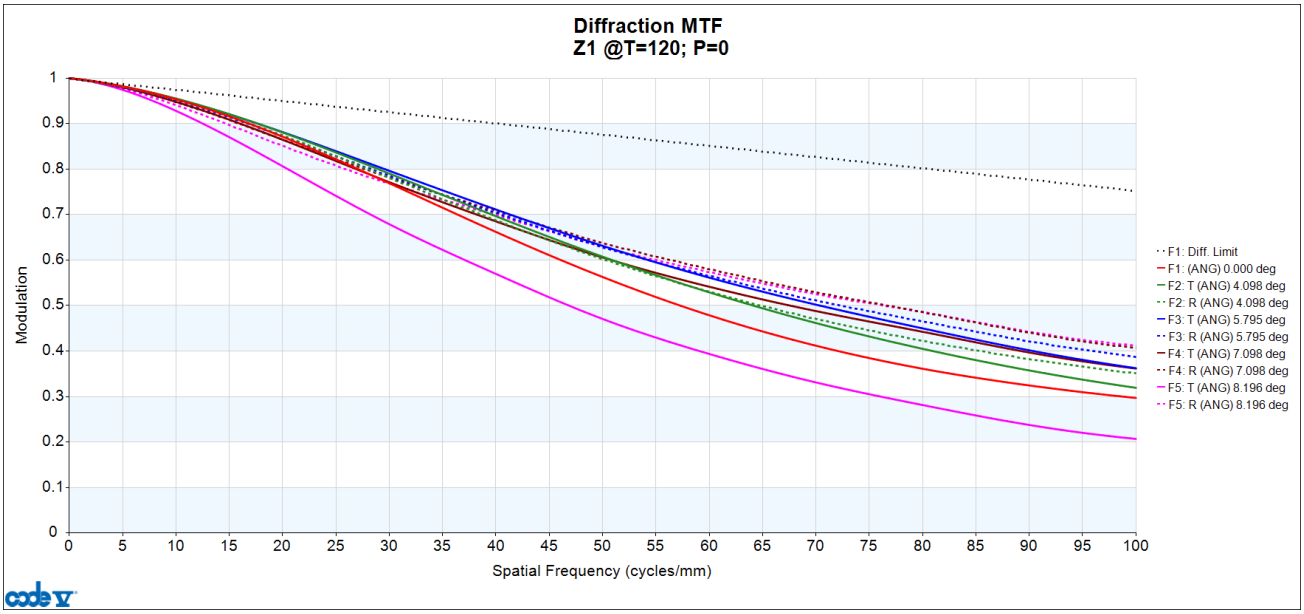

Figure 24: MTF (at T= -80, P = 0 mm Hg) for the design of Figure 16, assuming edge-cementing of elements.

Comparing these to Figures 17, 18, and 19, it can be seen that although the MTF at the extreme temperatures suffers a modest (though not catastrophic) loss. At the nominal fabrication temperature, the MTF is unchanged by this change in the mounting details. (This makes sense: if the temperature remains at the fabrication temperature, it does not matter how the elements are held.)

It should be noted that what caused the drop in MTF was a *change* to the element mounting plan after the system was optimized. The drop in MTF could be fully recovered with a short optimization based on the updated mounting plan.

6. CONCLUSIONS

By carefully taking into account the thermo-optical constants, the coefficients of expansion, and the geometric details surrounding how the elements are mounted, we have demonstrated an optically athermalized design (relative to an all-aluminum housing) that remains stable over a 200 degree temperature range. The selection of glass types was an essential part of achieving thermal stability. Small details of the optomechanical design (such as whether the mount contacts the left side or the right side of each element) have a non-negligible influence on the final performance of the system. We investigated a change from a face-seating approach to an approach using cement around the periphery of an optical element and determined that this change, when not accompanied by a subsequent reoptimization, was sufficient to cause a noticeable degradation of the image quality.

REFERENCES

[1] Lloyd, J.M., [Thermal Imaging Systems], McGraw-Hill Publishers, New York, 257-267 (1975).

[2] Rogers, P.J. and Roberts, M., 'Thermal Compensation Techniques' in [Handbook of Optics Vol I], McGraw-Hill Publishers, New York, 39.1-39.17 (1995).

[3] Gross, H., Blechinger, F., and Achtner, B. 'Infrared Systems' in [Handbook of Optical Systems Vol IV], Wiley-VCH Verlag GmbH & Co. Weinheim, 416-418 (2008).

[4] Rogers, J. R., "Passive athermalization: required accuracy of the thermo-optical coefficients," International Optical Design Conference 2014, *Proc. SPIE*. 9293, (2014)

[5] CODE V is a registered trademark of Synopsys, Inc.

[6] https://www.nist.gov/mml/acmd/aluminum-6061-t6-uns-aa96061